Surface Fluorinated Microsized-TiO$_2$ for Formulation of Self-Cleaning Cement

Saini, Anil; Ratan, Jatinder Kumar*+

Department of Chemical Engineering, Dr. B R Ambedkar National Institute of Technology,
Jalandhar-144 011, Punjab, INDIA

ABSTRACT: *The use of nanosized-Titanium dioxide (n-TiO$_2$) for the formulation of self-cleaning cement has the associated drawbacks of nano-toxicity, higher cost, and agglomeration in the cementitious material. These drawbacks can be avoided by the replacement of n-TiO$_2$ with microsized TiO$_2$ (m-TiO$_2$). However, m-TiO$_2$ is less photocatalytically active as compared to n-TiO$_2$. Therefore, in the present work, surface fluorination of m-TiO$_2$ has been studied to enhance its photocatalytic activity for the formulation of self-cleaning white cement. The commercially available m-TiO$_2$ (average size 40 μm) was surface fluorinated using aqueous solutions of different molar concentrations of NaF (sodium fluoride) such as 10, 50, and 100 mmol/dm^3. The surface fluorinated m-TiO$_2$ was analyzed using Diffuse Reflectance (DRS) Spectroscopy, PhotoLuminescence (PL) spectroscopy, and X-Ray diffraction (XRD) analysis to observe the improvement in the physiochemical properties and photocatalytic characteristics. Further, the surface fluorinated m-TiO$_2$ along with calcined dolomite was utilized for the formulation of self-cleaning white cement. The hence prepared self-cleaning cement was cast into cement slabs, which were then characterized by Diffuse Reflectance Spectroscopy (DRS) and Energy Dispersive Spectroscopy (EDS). The self-cleaning ability and photocatalytic activity of the as-prepared cement slabs were evaluated through Rhodamine B (RhB) degradation test. It has been found that the use m-TiO$_2$, which was surface fluorinated using 10 mmol/dm^3 solution of NaF, remarkably enhanced the photocatalytic performance of the self-cleaning cement.*

KEYWORDS: *Titanium dioxide; Self-cleaning cement; Photocatalytic activity; Photocatalysis; Surface fluorination; White cement.*

INTRODUCTION

Advanced Oxidation Processes (AOPs) have been widely studied for indoor and outdoor environmental remediation [1-4]. In AOPs, highly reactive oxygen species are generated and utilized for the oxidation of pollutants present in water and air. Based on the source of reactive oxygen species, AOPs are classified as photolysis, photocatalysis, photo-Fenton, ozonation, and UV/H$_2$O$_2$ processes etc. [1,5-6]. Among all the AOPs, extensive research work has been conducted on photocatalysis during the last decade [7]. Photocatalysis involves the generation of highly reactive oxygen species by activating a photocatalyst using a light source [8]. Nanostructured-TiO$_2$ (n-TiO$_2$) has been proven to be a remarkable photocatalyst because of its high photocatalytic activity,

chemical and biological inertness, photostability, and relative availability. These properties of n-TiO_2 offer applications in water splitting and purification, solar cells, sensors, antimicrobial activity, air depolluting, self-cleaning, and antifogging [9-11].

In the field of building materials, self-cleaning cement has been synthesized by including n-TiO_2 in the formulation of cement. Self-cleaning cement is an environmentally friendly composite material with multifunctional attributes such as self-cleaning activity, depolluting properties, and antimicrobial characteristics [12-13]. The porous structure of hardened self-cleaning cement offers an effective contact between n-TiO_2 and the target pollutants present in the environment, thus, facilitating the photocatalytic oxidation of the pollutants in the presence of sunlight. However, the use of n-TiO_2 in the formulation of self-cleaning cement has associated disadvantages of nano-toxicity, higher cost, and agglomeration in the cementitious material [14-15]. The use of microsized-TiO_2 (m-TiO_2) in place of n-TiO_2 in the formulation of self-cleaning cement can help to lessen the above-mentioned drawbacks. However, m-TiO_2 is less photocatalytically active as compared to n-TiO_2 due to a smaller surface area, higher band gap, and increased recombination rate. As such, the use of m-TiO_2 in the formulation of self-cleaning cement may lead to a reduction in photocatalytic activity, thus, reducing the self-cleaning and depolluting ability of the resultant cement material. So improvement in the photocatalytic activity of m-TiO_2 is the key issue for its practical application in the production of self-cleaning cement [16].

Thus far, fluorination of n-TiO_2 has been expansively studied in the literature to improve its various characteristic features for better photocatalytic performance [17-23]. There are two kinds of fluorination processes used for improving the properties of n-TiO_2; *(i)* doping of the fluorine (F) elements into the lattice structure to change the crystallinity, band gap, and recombination rate; and *(ii)* adsorbing the fluoride (F^-) ions on the surface to alter the surface charge and polarity leading to improved charge carrier transfer and recombination, and enhanced pollutant adsorption [17]. In surface fluorination, adsorption of F^- ions on Ti (titanium) atoms takes place, while in F doping, F^- ions are substituted with O_2^- lattice ions in the crystal structure of TiO_2 [16, 24-27].

Since the photocatalytic reactions are surface reactions, the surface fluorination of m-TiO_2 can also effectively enhance its photocatalytic performance by modifying the surface charge, surface acidity, surface functional groups, and crystalline phase content. However, the literature studies are focused on surface fluorination of n-TiO_2 only, and to the best of our knowledge, the surface fluorination of m-TiO_2 of the average size of 40 μm has never been studied. Also, the incorporation of such surface fluorinated m-TiO_2 along with calcined dolomite in the cement formulation, for improvement in the photocatalytic performance of the resultant self-cleaning cement, needs further investigation. Therefore, the present study deals with the various aspects of the surface fluorination of m-TiO_2 (40 μm), and its application in the formulation of self-cleaning white cement for the enhancement of photocatalytic activity. The average size of different cement ingredients used in the present study was 42-45 μm. Therefore, m-TiO_2 (40 μm) of almost a similar size to the cement ingredients was utilized in the present study for the formulation of self-cleaning white cement to; (a) provide a uniform mixing (without agglomeration) in the cement powder; (b) diminish nano-toxicity during the synthesis and use of resultant self-cleaning cement and (c) maintain the production cost at an economical level.

EXPERIMENTAL SECTION
Materials and Methods
Materials

Sodium fluoride (NaF, 99% w/w) and nitric acid (HNO_3, 70% v/v) were purchased from Himedia and SDFCL, respectively. The clinker of white cement (containing 3% gypsum) was cordially provided by JK White Cement Works, Gotan (India). The mean size of the clinker was 42 μm. Titanium dioxide (BTA-100) was purchased from BMC Pvt. Ltd. (Chennai). BTA-100 was containing 97-98 % titanium dioxide, and the average particle size was 40 μm. Dolomite was obtained from Jodhpur area of northern India. The dolomite was having a mean size of 45 μm. Rhodamine-B, an organic dye, was purchased from HiMedia Laboratories Pvt. Ltd. (Mumbai).

Surface fluorination of m-TiO2

An inexpensive precursor i.e. NaF was chosen for surface fluorination of m-TiO_2 so that the process of formulation of self-cleaning cement be kept facile and economical.

The powdered NaF weighing 37.7, 188.5, and 377 mg was dissolved separately in 90 mL of distilled water in each case to prepare 10, 50, and 100 $mmol/dm^3$ of aqueous NaF solutions, respectively. The HNO_3 (70%) was diluted by mixing 1mL of it in 100 mL of distilled water. The diluted HNO_3 was added dropwise to 10, 50, and 100 $mmol/dm^3$ of NaF solutions to maintain the pH at 3. Then, 3g of $m-TiO_2$ were suspended in each of the above-mentioned NaF solutions and constantly stirred at 1000 rpm for 1.5 h at room temperature. After the stirring, the mother liquor was decanted, and the fluorinated $m-TiO_2$ was washed two times with distilled water to remove any unreacted NaF. The fluorinated $m-TiO_2$ was then dried in the oven at 40 °C overnight.

The samples obtained by surface fluorination of $m-TiO_2$ with 10, 50, and 100 $mmol/dm^3$ of NaF solutions were named $F10/m-TiO_2$, $F50/m-TiO_2$, and $F100/m-TiO_2$, respectively. The bare $m-TiO_2$ with no surface fluorination was coded as $F0/m-TiO_2$.

Characterization analysis

The self-cleaning white cement obtained using $F10/m-TiO_2$ sample showed the best photocatalytic activity in the present work (refer to the Results and Discussion section) in the present study. Therefore, characterization was focused on $F10/m-TiO_2$ along with non-fluorinated $F0/m-TiO_2$ for comparative analysis. Diffuse Reflectance Spectra (DRS) were obtained using UV–vis spectrophotometer (UV-2600, Shimadzu), and the X-Ray Diffraction (XRD) patterns were obtained on Bruker D8 X-ray diffractometer (Cu Kα radiations, Λ = 1.54060 Å), operated at 45kV and 40 mA. Photoluminescence (PL) spectra were recorded at room temperature at an excitation wavelength of 230 nm and emission range of 350-360 nm by using a Perkin Elmer spectrofluorometer, (LS45, USA).

Preparation and characterization of self-cleaning cement slabs

The weight percentage of various dry ingredients used for preparing different self-cleaning cement slabs for the present study was 87% clinker, 10% calcined dolomite (co-adsorbent), and 3% $m-TiO_2$. The cement slabs prepared by using $F0/m-TiO_2$, $F10/m-TiO_2$, $F50/m-TiO_2$, and $F100/m-TiO_2$ were nomenclatured as CT0, CTF10, CTF50, and CTF100, respectively. In the present work,

57 g of cement powder from each sample was hydrated and mixed with 22.8 g of water to form the cement paste. The cement paste of each sample was cast in 98 mm diameter petri dish and cured for one day at room temperature. Water was sprinkled manually on the cement samples at an interval of 2 h for the initial period of 8 h of curing. Cement discs of thickness 5 mm were obtained in each case after the casting process. The cement discs were then cut into smaller square slabs of the same surface area (645 mm^2) for further use in the present study. Diffuse reflectance spectra (DRS) of all the cement slabs were obtained to evaluate their light absorption characteristics, which is a significant parameter of any photocatalytic surface. Field Emission-Scanning Electron Microscope (FE-SEM; Carl Zeiss Ultra Plus) along with Energy Dispersive X-ray Spectroscopy (EDS) was used to map the titanium (Ti) and fluorine (F) particles on the surface of the cement slabs.

Photocatalytic activity

The self-cleaning ability of the cement slabs was evaluated based on the photocatalytic activity test. A volume of 50 μL of aqueous Rhodamine B (RhB) solution (100 mg/L) was uniformly coated on the surface of the prepared cement slabs using the doctor blade technique [28]. The cement slabs were then irradiated for a period of 8h with 1.4 mW/cm^2 of UVA light to simulate daylight with illumination in the wavelength range of 320-400 nm. The discoloration of RhB (λ_{max} at 554 nm) on the surface of the cement slabs due to photocatalytic action was measured using a UV-Visible spectrophotometer (UV-2600, Shimadzu).

RESULTS AND DISCUSSION
Characterization results

The Diffuse-Reflectance Spectra (DRS) of the bare $m-TiO_2$ ($F0/m-TiO_2$) and surface fluorinated $m-TiO_2$ ($F10/m-TiO_2$) were obtained and compared as shown in Fig.1. The $F10/m-TiO_2$ has shown significantly better light absorption characteristics as compared to $F0/m-TiO_2$ throughout the radiation range of 200-800 nm. The $F10/m-TiO_2$ has depicted almost 95% of energy absorbance in the UV range of 200-320 nm. In the UVA region of 320-400 nm, the average reflectance of energy was observed to be 51% in the case of $F10/m-TiO_2$, indicating better light absorption characteristics in this particular wavelength range, which was also utilized in the photocatalytic activity test for irradiation of cement slabs. The improved
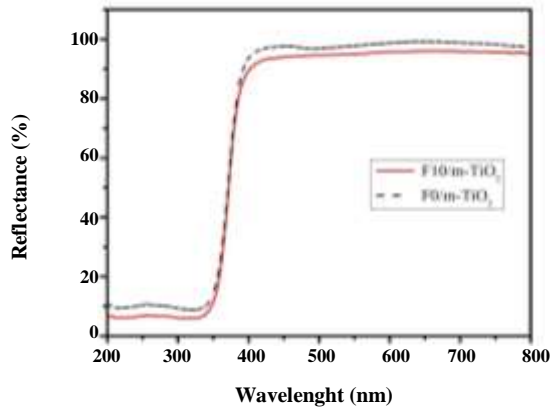
Fig. 1: Diffuse reflectance spectra of F0/m-TiO₂ and F10/m-TiO₂ .

Fig. 2: Photoluminescence spectra of F0/m-TiO₂ and F10/m-TiO₂ .

light-absorption characteristics portrayed by F10/m-TiO₂ are indicative of comparatively enhanced photocatalytic activity.

The Photoluminescence spectra of F0/m-TiO₂ and F10/m-TiO₂ were obtained to evaluate the effect of surface fluorination on the recombination of charge carriers. It is evident from the spectra (Fig. 2) that the PL emission intensity of F10/m-TiO₂ is notably lower than that of F0/m-TiO₂. This observation indicates that surface fluorination has retarded the recombination rate in the bulk of m-TiO₂, which is an indirect gesture of improved photocatalytic ability.

The crystal structure of F0/m-TiO₂ and F10/m-TiO₂ were analyzed and compared by XRD technique. Fig. 3 portrays the XRD patterns and Table 1 represents the structural properties of both samples. The crystalline size (d) was calculated by the use of Eq.(1), and the anatase phase percentage ($A\%$) was determined using Eq. (2) [29]:

$$d = \frac{0.9 \times \lambda}{FWHM \times \cos\theta} \tag{1}$$

$$A(\%) = \frac{100}{1 + 1.265 \left(I_R / I_A \right)} \tag{2}$$

Where λ is the X-ray wavelength, FWHM is the full width at half maximum height for the anatase (1 0 1) peak, θ is the Bragg's diffraction angle for the same peak, I_R is the intensity of the largest rutile peak, and I_A is the intensity of the largest anatase peak.

The XRD pattern (Fig. 3) depicts the peaks for anatase (A) and rutile (R) phases, which confirms the simultaneous presence of both phases in F0/m-TiO₂ and F10/m-TiO₂.
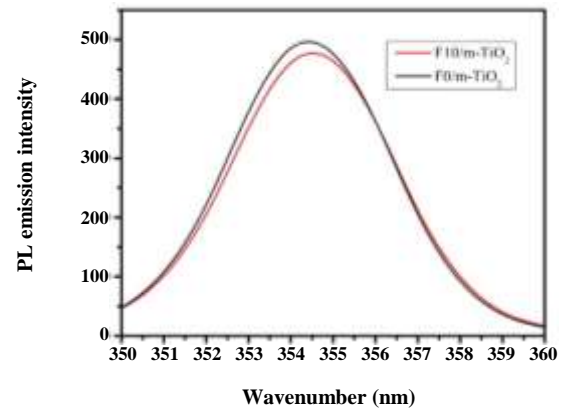
There is no signal found for the occurrence of any phase containing the F element in fluorinated sample F10/m-TiO₂, which authenticates that no doping of fluoride ion took place into the lattice structure of m-TiO₂ during the surface fluorination process. The slight shift and decrease in the intensity of the peaks of anatase and rutile phase have been observed upon surface fluorination. A change in various crystal features such as crystalline size, phase content, d-spacing and lattice parameters (Table 1) have also been observed after the surface fluorination of bare m-TiO₂.

Photocatalytic activity

The self-cleaning property of the cement slabs was assessed by their photocatalytic activity to reduce the color of RhB dye coated on the surface. Fig. 4 shows the percentage color reduction of the coated dye with respect to time under simulated daylight for different cement slabs. The color reduction of RhB is an indirect measure of its degradation and decomposition. As obvious, the cement slab CTF10 revealed the best photocatalytic activity with 75% degradation of RhB after 8h of UVA illumination. Degradation of 58, 65, and 59% of RhB was observed for the same period of illumination in the case of CT0, CTF50, and CTF100 cement slabs, respectively. The observed degradation of RhB is a measure of the self-cleaning performance of the cement samples. All the cement slabs showed higher photocatalytic degradation rates during the first 2h, which gradually decreased towards the end of the experiment. This behavior depicted that the photocatalytic degradation of RhB followed the pseudo-first-order kinetics according to the Langmuir-Hinshelwood model [30]. Fig. 5 depicts the visual images

Table 1: Structural features of F0/m-TiO₂ and F10/m-TiO₂.

Sample	Crystalline size (nm) at peak (1 0 1)	Phase content (A/R)%	d-spacing (Å)	Lattice parameter for A (Å)	Lattice parameter for R (Å)
F0/m-TiO₂	115	(94/6)	3.529	a = b = 3.789 c = 9.537	a = b = 4.602 c = 2.965
F10/m-TiO₂	80	(91/9)	3.514	a = b = 3.785 c = 9.52	a = b = 4.594 c = 2.959
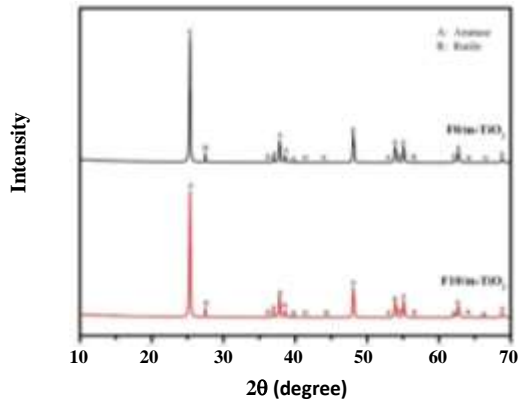
Fig. 3: XRD patterns of F0/m-TiO₂ and F10/m-TiO₂ .
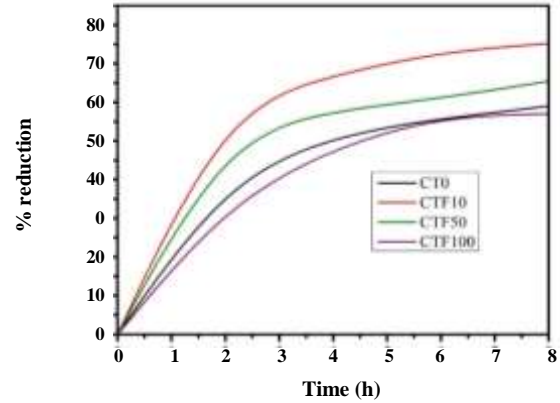
Fig. 4: Percentage color reduction of coated dye.

(a)　　　　　　　　　　　　　　　　　　　　　　(b)
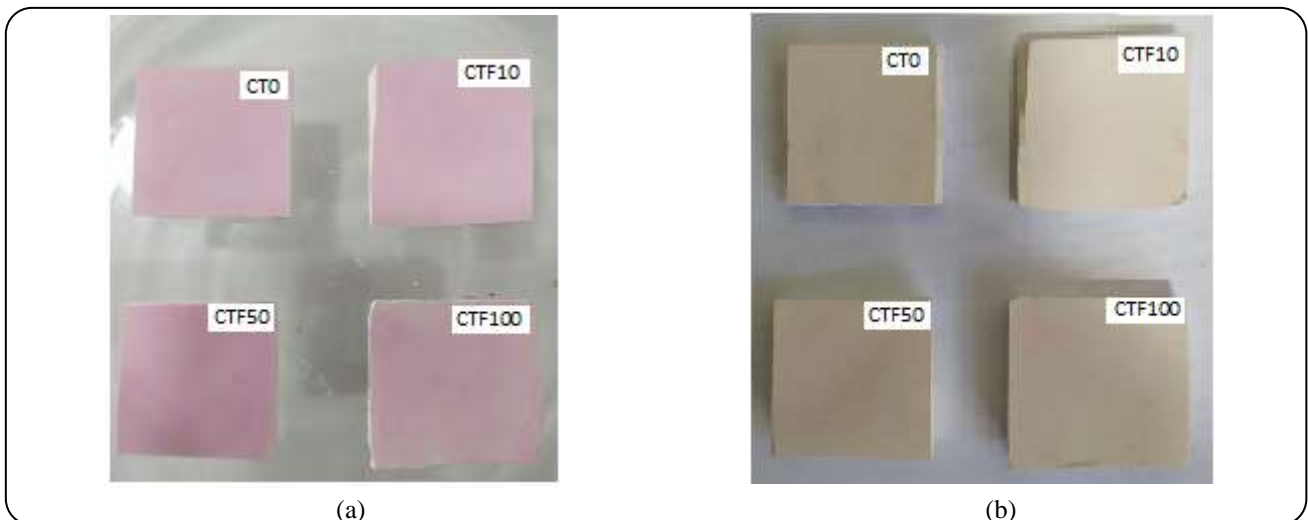
Fig. 5: Photographs of the cement slabs (a) before and (b) after the photocatalytic activity test.

of all the cement slabs before and after the photocatalytic activity test. The visual examination of the surfaces of the cement slabs indicates that the dye coated on the surface of CTF10 has been efficiently removed as compared to other slabs due to better photocatalytic activity.

The key reason for the best photocatalytic performance of CTF10 sample among all the tested samples is that it contains m-TiO₂ (F10/m-TiO₂), which is optimally fluorinated with 10 mmol/dm³ of NaF solution. Surface

fluorination takes place by the exchange of F⁻ and OH⁻ groups on the surface of m-TiO₂, therefore the surface of the fluorinated m-TiO₂ is negatively charged has lower adsorption for negatively charged molecules such as water, and more adsorption for positively charged molecules such as RhB (existing as RhB⁺ ions in the aqueous solution), which provides better photocatalytic oxidation of the dye [16, 31-32]. Moreover, the highly electronegative F causes electron accumulation near ≡Ti-F bond hindering
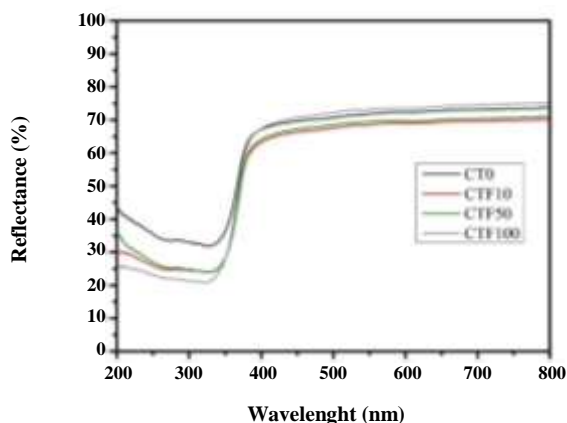
Fig. 6: Diffuse reflectance spectra of cement slabs.

the electron (e^-) transfers to O_2 on the surface of m-TiO₂ retarding the recombination rate [17, 19-20, 33-35]. Further, the chemisorbed fluoride favors the transfer of valence band holes (h_{vb}^+) to the interface resulting in increased formation of hydroxyl radicals ($^•OH$), which further speed up the photocatalytic oxidation of RhB [17].

However, the surface of m-TiO₂ fluorinated with higher concentrations (50 mmol/dm³ and 100 mmol/dm³) of NaF solution gets extra negatively charged. Therefore, the enhanced electrostatic repulsion between the negatively charged surface of m-TiO₂ and electron (e^-) more seriously inhibits the transfer of photogenerated electrons to the surface and consequently increases the recombination rate of the charge carriers in the m-TiO₂ bulk phase, thus depressing the photocatalytic activity [16, 27, 31]. Thus, the cement slabs CTF50 and CTF100 which contains F50/m-TiO₂, and F100/m-TiO₂ in their formulation showed lower photocatalytic activity for the degradation of RhB. The cement slab CT0 with no fluorinated m-TiO₂ showed the lowest photocatalytic activity due to obvious reasons.

The results of the photocatalytic activity test were validated and supported through the characterization of the cement slabs. Fig. 6 shows the Diffuse Reflectance Spectra (DRS) of all the cement slabs before the coating of RhB. It is obvious that CTF10 has shown the minimum reflectance or maximum absorption of light in the UVA region (320-400 nm), which may be attributed to the presence of optimally fluorinated m-TiO₂. The more the absorption of light energy, the better will be the photocatalytic activity and self-cleaning ability. Thus, the cement slab CTF10 has shown better photocatalytic performance as compared to other

cement slabs. A significant phenomenon observed from the DRS of cement slabs is that the average reflectance in the studied UVA range of 320-400 nm for CTF10 slab (made from F10/m-TiO₂) was 44% , while it was found to be 51% for pure F10/m-TiO₂ (see Fig. 1). Similarly, in the visible region (400-800 nm), CTF10 showed relatively lesser reflectance of *ca.* 65%, while pure F10/m-TiO₂ showed more reflectance of *ca.* 93%. The lesser reflectance (or more absorption) of light in the case of cement, slabs may be attributed to the collective light-trapping effect of fluorinated m-TiO₂, calcined dolomite (co-adsorbent), and cement matrix.

Fig. 7 shows the EDS mapping of F and Ti on the surface of CT0 and CTF10 cement slabs before coating RhB. The red spots in the image represent the Ti particles (m-TiO₂) and the green dots indicate the F particles (fluorinated m-TiO₂) on the surface of the cement slabs CT0 and CTF10. There is no F present on the surface of CT0 slabs because no surface fluorination was performed on m-TiO₂ used in this slab. It can be visualized physically from the EDS images that m-TiO₂ is more uniformly distributed (without agglomeration) on the surface of CTF10 as compared to CT0. Fluorinated m-TiO₂ is also found uniformLy distributed all around the surface of CTF10. The visual examination of the EDS images portrays that relatively more m-TiO₂ (bare and fluorinated) was available on the surface of CTF10 slab to provide better self-cleaning ability. The higher concentration of bare and fluorinated m-TiO₂ on the surface of cement slab CTF10 led to better light absorption characteristics and photocatalytic activity, which ultimately enhanced the degradation of RhB dye.

CONCLUSIONS

The m-TiO₂ was surface fluorinated using various concentrations of an aqueous solution of NaF such as 10, 50, and 100 mmol/dm³. The characterization study of surface fluorinated m-TiO₂ depicted an improvement in its physiochemical properties and photocatalytic characteristics. There was no indication of doping of fluoride anion into the crystal lattice of m-TiO₂, and only the chemisorption of fluoride ions on the surface of m-TiO₂ was observed. The self-cleaning white cement is formulated by 87% clinker, 10% calcined dolomite, and 3% m-TiO₂ (fluorinated using 10 mmol/dm³ solution of NaF) has been found to show enhanced self-cleaning
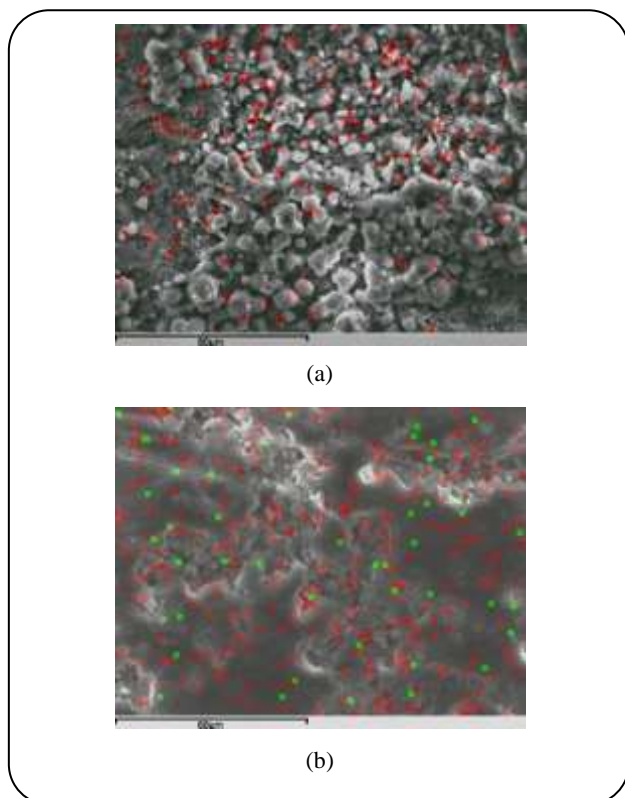
Fig. 7: SEM-EDS image of (a) CT0 and (b) CTF10 cement slabs.

ability and photocatalytic activity with 75% degradation of Rhodamine B dye. This study clearly demonstrated that the use of m-TiO₂ (optimally surface fluorinated with 10 mmol/dm³ aqueous solution of NaF) for the formulation of self-cleaning cement remarkably enhances the photocatalytic performance due to reduced recombination rate, effective transfer of holes to the surface, and improved light absorption characteristics.

REFERENCES

[1] Gatto S., Sansotera M., Persico F., Gola M., Pirolaa C., Panzeri W., Navarrini, Bianchi C.L., Surface Fluorination on TiO₂ Catalyst Induced by Photodegradation of Perfluorooctanoic Acid, *Catal*., **241**: 8–14 (2015).

[2] Flores C., Ventura F., Martin-Alonso J., Caixach J., Occurrence of Perfluorooctane Sulfonate (PFOS) and Perfluorooctanoate (PFOA) in N.E. Spanish Surface Waters and their Removal in a Drinking Water Treatment Plant that Combines Conventional and Advanced Treatments in Parallel Lines, *Sci. Total Environ.*, **461–462:** 618–626 (2013).

[3] Khan J.., Tariq M., Muhammad M., Mehmood M.H., Ullah I. Application of Photo-Fenton System(UV/ H₂O₂/ Fe²⁺) for Efficient Decolorization of Azo-Dye Acid Yellow 17 in Aqueous Solution, *Iran. J. Chem. Chem. Eng. (IJCCE),* **39(1)**:127-140 (2020).

[4] Lutze H., Panglisch S., Bergmann A., Schmidt T.C., Treatment Options for the Removal and Degradation of Polyfluorinated Chemicals, in: T.P. Knepper, F.T.Lange (Eds.), Polyfluorinated Chemicals and Transformation Products, *Hdb. Env. Chem.,* Springer, Heidelberg, pp 103–125 (2012).

[5] Neda S.T., Narjes K., Mohsen M.G., Photocatalytic Degradation of Ethylbenzene by Nano Photocatalyst in Aerogel form Based on Titania, *Iran. J. Chem. Chem. Eng. (IJCCE)*, **40(2):** 525-537 (2021).

[6] Mills A., Hunte S. L., An Overview of Semiconductor Photocatalysis, *Photochem J. Photobiol., A: Chem.,* **108**: 1–35 (1997).

[7] Samira K., Ebrahim A., Lobat T., Leila S., Comparing Nanocomposites of TiO₂/SBA-15and TiO₂/GO for Removal of Phenol out of Aqueous Solutions, *Iran. J. Chem. Chem. Eng. (IJCCE),* **39(5):** 121-130 (2020).

[8] Meng C., Dong P., Tian H., Cheng T., Li J., Liu Y., Yang X., Xie M., Chen X., Xi X., Photocatalytic Concrete Paving Block Reinforced by TiO₂ Nanotubes for NO Removal, *J. Mater. Sci.,* **55**: 14280–14291 (2020).

[9] Karapati S., Giannakopouloua T., Todorovaa N., Boukos N., Antiohos S., Papageorgioub D., Chaniotakis E., Dimotikali D., Trapalis C., TiO₂ Functionalization for Efficient NOx Removal in Photoactive Cement, *Appl. Surf.Sci.,* **319**: 29-36 (2014).

[10] Zahra S., Effat I., Ali M.L., Meisam T. M., Lead Adsorption onto Surface Modified Nano Titania: Kinetic and Thermodynamic Studies, *Iran. J. Chem. Chem. Eng. (IJCCE)*, **39(6)**: 105-119 (2020).

[11] Nisha T., Padmanabhan, Honey J., Review: Titanium Dioxide Based Self-Cleaning Smart Surfaces, *J. Environ. Chem. Eng.,* **8**: 104211 (2020).

[12] Akono Ange-Therese, Effect of Nano-TiO₂ on C–S–H Phase Distribution within Portland Cement Paste, *J. Mater. Sci.,* **55**:11106–11119 (2020).

[13] Ganji N., Allahverdi A., Naeimpoor F., Mahinroosta M., Photocatalytic Effect of Nano-TiO₂ loaded Cement on Dye Decolorization and Escherichia Coli Inactivation under UV Irradiation, *Res. Chem. Intermed*., **42**:5395–5412 (2016).

[14] Saini A., Arora I., Ratan J. K., Photo-induced Hydrophilicity of Microsized-TiO₂ based Self-Cleaning Cement, *Mater. Lett.,* **260**: 126888 (2020).

[15] Ratan J.K., Saini A., Enhancement of Photocatalytic Activity of Self-Cleaning Cement, *Mater. Lett.,* **244**: 178–181 (2019).

[16] Chen Y., Chen F., Zhang J., Effect of Surface Fluorination on the Photocatalytic and Photo-Induced Hydrophilic Properties of Porous TiO₂ Films, *Appl. Surf.Sci.*, **255**: 6290–6296 (2009).

[17] Shayegan Z., Lee C.-S., Haghighat F., Effect of Surface Fluorination of P25-TiO₂ Coated on Nickel Substrate for Photocatalytic Oxidation of Methyl Ethyl Ketone in Indoor Environments, *J. Environ. Chem. Eng.,* **7**: 103390 (2019).

[18] Shayegan Z., Lee C.-S., Haghighat F., Review: TiO₂ Photocatalyst for Removal of Volatile Organic Compounds in Gas Phase, *Chem. Eng. J*., **334**: 2408–2439 (2018).

[19] Chiarello G.L., Dozzi M.V., Scavini M., Grunwaldt J.-D., Selli E., One Step Flame-Made Fluorinated Pt/TiO2 Photocatalysts for Hydrogen Production, *Appl. Catal. B.,* **160–161**: 144–151 (2014).

[20] Shayegan Z., Haghighat F., Lee C.-S., Bahloul A., Huard M., Effect of Surface Fluorination of P25-TiO₂ on Adsorption of Indoor Environment Volatile Organic Compounds, *Chem. Eng. J.,* **346**: 578–589 (2018).

[21] Laciste M.T., de Luna M.D.G., Tolosa N.C., Lu M.-C., Degradation of Gaseous Formaldehyde *via* Visible Light Photocatalysis using Multi-Element Doped Titania Nanoparticles, *Chemosphere*, **182**: 174–182 (2017).

[22] Liu S.-H., Lin W.-X., A Simple Method to Prepare g-C3N4-TiO₂/waste Zeolites as Visible-light-Responsive Photocatalytic Coatings for Degradation of Indoor Formaldehyde, *J. Hazard. Mater.,* **368**: 468–476 (2019).

[23] Mirzaei A., Haghighat F., Chen Z., Yerushalmi L., Sonocatalytic Removal of Ampicillin by Zn(OH)F: Effect of Operating Parameters, Toxicological Evaluation and Byproducts Identification, *J. Hazard. Mater.,* **375**: 86–95 (2019).

[24] Dozzi M. V., Selli E., Effects of Phase Composition and Surface Area on the Photocatalytic Paths on Fluorinated Titania, *Catal.,* **206**: 26–31 (2013).

[25] Mrowetz M., Selli E., Enhanced Photocatalytic Formation of Hydroxyl Radicals on Fluorinated TiO₂, *Phys. Chem. Chem. Phys.,* **7**: 1100 (2005).

[26] Minero C., Mariella G., Maurino V., Vione D., Pelizzetti E., Photocatalytic Transformation of Organic Compounds in the Presence of Inorganic Ions. 2. Competitive Reactions of Phenol and Alcohols on a Titanium Dioxide−Fluoride System, *Langmuir*, **16**: 8964–8972 (2000).

[27] Park H., Choi W., Phys J., Effects of TiO₂ Surface Fluorination on Photocatalytic Reactions and Photoelectrochemical Behaviors, *Chem, J. Phys. Chem.* B., **108**: 4086–4093 (2004).

[28] Le H.V., Pham P.T., Le L.T., Nguyen A.D., Tran N.Q., Tran P.D., Fabrication of Tungsten Oxide Photoanode by Doctor Blade Technique and Investigation on its Photocatalytic Operation Mechanism, *Int. J. Hydrog. Energy*, 46: 22852-22863 (2021).

[29] Natarajan K., Natarajan T.S., Bajaj H.C., Tayade R.J., Photocatalytic Reactor based on UV-LED/TiO₂ Coated Quartz Tube for Degradation of Dyes, *Chem. Eng. J.,* **178**: 40– 49 (2011).

[30] Mahmood A., Wang X., Xie X., Sun J., Degradation Behavior of Mixed and Isolated Aromatic Ring Containing VOCs: Langmuir-Hinshelwood Kinetics, Photodegradation, In-Situ FTIR and DFT Studies, *J. Environ. Chem. Eng*., 105069 (2021).

[31] Vohra M.S., Kim S., Choi W., Effects of Surface Fluorination of TiO₂ on the Photocatalytic Degradation of Tetramethylammonium, *J. Photochem. Photobiol. A.,* **160**: 55–60 (2003).

[32] Chiarello G.L., Dozzi M.V., Scavini M., Grunwaldt J.-D., Selli E., One Step Flame-made Fluorinated Pt/TiO₂ Photocatalysts for Hydrogen Production, *Appl. Catal. B.,* **160–161**:144–151 (2014).

[33] Monllor-Satoca D., Gómez R., Electrochemical Method for Studying the Kinetics of Electron Recombination and Transfer Reactions in Heterogeneous Photocatalysis: The Effect of Fluorination on TiO₂ Nanoporous Layers, *J. Phys. Chem. C.,* **112**: 139–147 (2008).

[34] Wu H., Ma J., Li Y., Zhang C., He H., Photocatalytic Oxidation of Gaseous Ammonia over Fluorinated TiO₂ with Exposed (001) Facets, *Appl. Catal. B.,* **152–153**: 82–87 (2014).

[35] Vijayabalan A., Selvam K., Velmurugan R., Swaminathan M., Photocatalytic Activity of Surface Fluorinated TiO₂-P25 in the Degradation of Reactive Orange 4, *J. Hazard. Mater.,* **172**: 914–921 (2009).